Rearrangement of a polar core provides a conserved mechanism for constitutive activation of class B G protein-coupled receptors

Received for publication, February 23, 2017, and in revised form, March 20, 2017 Published, Papers in Press, March 29, 2017, DOI 10.1074/jbc.M117.782987

Yanting Yin[‡§¶], Parker W. de Waal[§], Yuanzheng He[§], Li-Hua Zhao[‡], Dehua Yang[‖], Xiaoqing Cai[‖], Yi Jiang[‡], Karsten Melcher[§], Ming-Wei Wang[‖1], and H. Eric Xu[‡§¶2]**

*From the [‡]Van Andel Research Institute - Shanghai Institute of Materia Medica (VARI-SIMM) Center, Center for Structure and Function of Drug Targets, The CAS Key Laboratory of Receptor Research, Shanghai Institute of Materia Medica, Chinese Academy of Sciences (CAS), Shanghai 201203, China, the [§]Laboratory of Structural Sciences and Laboratory of Structural Biology and Biochemistry, Van Andel Research Institute, Grand Rapids, Michigan 49503, the [¶]University of Chinese Academy of Sciences, Number 19A Yuquan Road, Beijing 100049, China, [‖]The National Center for Drug Screening and the CAS Key Laboratory of Receptor Research, Shanghai Institute of Materia Medica, Chinese Academy of Sciences, Shanghai 201203, China, and the **School of Pharmacy, Fudan University, 826 Zhangheng Road, Shanghai 201203, China*

Edited by Henrik G. Dohlman

The glucagon receptor (GCGR) belongs to the secretin-like (class B) family of G protein-coupled receptors (GPCRs) and is activated by the peptide hormone glucagon. The structures of an activated class B GPCR have remained unsolved, preventing a mechanistic understanding of how these receptors are activated. Using a combination of structural modeling and mutagenesis studies, we present here two modes of ligand-independent activation of GCGR. First, we identified a GCGR-specific hydrophobic lock comprising Met-338 and Phe-345 within the IC3 loop and transmembrane helix 6 (TM6) and found that this lock stabilizes the TM6 helix in the inactive conformation. Disruption of this hydrophobic lock led to constitutive G protein and arrestin signaling. Second, we discovered a polar core comprising conserved residues in TM2, TM3, TM6, and TM7, and mutations that disrupt this polar core led to constitutive GCGR activity. On the basis of these results, we propose a mechanistic model of GCGR activation in which TM6 is held in an inactive conformation by the conserved polar core and the hydrophobic lock. Mutations that disrupt these inhibitory elements allow TM6 to swing outward to adopt an active TM6 conformation similar to that of the canonical β_2-adrenergic receptor complexed with G protein and to that of rhodopsin complexed with arrestin. Importantly, mutations in the corresponding polar core of several other members of class B GPCRs, including PTH1R, PAC1R, VIP1R, and CRFR1, also induce constitutive G protein signaling, suggesting that the rearrangement of the polar core is a conserved mechanism for class B GPCR activation.

The glucagon receptor (GCGR)[3] is one of the 15 members of the secretin-like family of class B G protein-coupled receptors (GPCRs) (1). Upon activation by binding to the 29-amino-acid hormonal peptide glucagon (GCG), GCGR stimulates both glycogenolysis and gluconeogenesis to maintain normal blood glucose levels (2). Given this central role in the regulation of both glucose metabolism and homeostasis, the modulation of GCGR signaling has become an active therapeutic target for treatment of type II diabetes and clinical obesity.

Class B GPCRs are defined by a large peptide-binding extracellular domain (ECD) comprising three conserved disulfide bonds (3–5) tethered to a canonical GPCR seven-transmembrane domain (TMD). Thus far, several structures of class B ECDs in complex with their peptide ligands have been determined by X-ray crystallography and NMR (3, 6–11). In addition, two structures of the GCGR TMD in complex with two different small molecule antagonists, NNC0640 and MK-0893, have been reported (12, 13). The ability of the GCGR ECD and TMD to fold independently into modular domain structures is

This work was supported by National Natural Science Foundation of China Grant 31300245 (to L. H. Z.) and in part by the Jay and Betty Van Andel Foundation, Ministry of Science and Technology of China Grants 2012ZX09301001, 2012CB910403, 2013CB910600, XDB08020303, and 2013ZX09507001; Amway (China); National Institutes of Health Grants DK071662 (to H. E. X.) and GM102545 and GM104212 (to K. M.); the Outstanding Young Scientist Foundation of CAS; the Youth Innovation Promotion Association of CAS; Shanghai Science and Technology Development Fund Grants 15DZ2291600 and 14431901200 (to M. W. W.); National Natural Science Foundation Grant 81373463 (to D. Y.); and the CAS-Novo Nordisk Research Fund (to D. Y.). The authors declare that they have no conflicts of interest with the contents of this article. The content is solely the responsibility of the authors and does not necessarily represent the official views of the National Institutes of Health.

This article was selected as one of our Editors' Picks.

[1] To whom correspondence may be addressed: National Center for Drug Screening, 189 Guo Shou Jing Rd., Shanghai 201203, China. Tel.: 86-21-50800598; Fax: 86-21-50800721; E-mail: mwwang@simm.ac.cn.

[2] To whom correspondence may be addressed: Laboratory of Structural Sciences, Center for Structural Biology and Drug Discovery, Van Andel Research Institute, Grand Rapids, MI 49503. Tel.: 616-234-5722; Fax: 616-234-5773; E-mail: Eric.Xu@vai.org.

[3] The abbreviations used are: GCGR, glucagon receptor; GPCR, G protein-coupled receptor; TM, transmembrane helix; AR, adrenergic receptor; GCG, glucagon; ECD, extracellular domain; TMD, transmembrane domain; GLP-1R, glucagon-like peptide-1 receptor; TEV, tobacco etch virus; tTA, tetracycline transactivator; CRF1R, corticotropin-releasing factor receptor type 1; PAC1R, pituitary adenylate cyclase-activating polypeptide type 1 receptor; PTH1R, parathyroid hormone 1 receptor; GCG-M, membrane-tethered GCG; CRE, cAMP-response element; VIP1R, vasoactive intestinal peptide receptor 1; VIP, vasoactive intestinal peptide; BETP, (4-(3-(benzyloxy) phenyl)-2-ethylsulfinyl-6-(trifluoromethyl)pyrimidine).

consistent with the "two-domain" model of class B GPCR hormone binding and activation (9). In the case of GCGR, the ECD has been proposed to be in close contact with the TMD in the ligand-free receptor, and this ECD-TMD contact is proposed to be part of a repression mechanism that keeps the receptor TMD in the inactive conformation (14, 15). Ligand binding to the GCGR ECD rearranges the ECD to a "stand up" position and releases the ECD repression of the TMD, which then results in receptor activation. Although the stand up activation model fits well with the general framework of the two-domain mechanism for ligand binding and activation of class B GPCR, it cannot explain the requirement of the ECD in activation of GCGR and GLP-1R (16). In these two receptors, we have shown that their ECDs play a much more direct role in the receptor activation in addition to their role in ligand binding (16). However, the absence of a fully activated class B GPCR structure has limited our mechanistic understanding of ligand binding and receptor activation for this important family of receptors.

In contrast to class B GPCRs, class A GPCRs are much better studied with respect to their mechanism of ligand binding and activation. The crystal structure of the β_2-adrenergic receptor (β_2AR)-bound G_s (17) reveals an opening of the cytoplasmic side of the TM bundle, exemplified by a dramatic outward movement of TM6 helix. Similar structural rearrangement has also been observed in the structure of rhodopsin bound to visual arrestin although with less pronounced outward movement of TM6 helix (18). The outward movement of TM6 is also commonly observed in many agonist-bound class A GPCR structures (19–22), thus serving as a hallmark of class A GPCR activation. Here, we present evidence that the conformational swing of TM6 could also serve as the general mechanism of class B GPCR activation. In the case of GCGR, TM6 is locked in the inactive conformation by a hydrophobic lock and a conserved polar core. Mutations that compromise these structural elements lead to constitutive activation of GCGR regardless of the presence of ligand or the GCGR ECD. Furthermore, mutations in the conserved polar code in several other members of class B GPCRs, including parathyroid hormone 1 receptor (PTH1R), pituitary adenylate cyclase-activating polypeptide type 1 receptor (PAC1R), vasoactive intestinal peptide receptor 1 (VIP1R), and corticotropin-releasing factor receptor type 1 (CRF1R), also result in constitutive activation, suggesting that the conformational swing of TM6 is also a common activation mechanism of class B GPCRs.

Results

Mutations at Phe-345 are sufficient to induce constitutive receptor activation

Incorporation of a cysteine at Phe-345 near the cytoplasmic side of TM6 has been shown to sensitize GCGR to the positive allosteric modulator BETP (4-(3-(benzyloxy)phenyl)-2-ethylsulfinyl-6-(trifluoromethyl)pyrimidine), leading to ligand-dependent positive allosteric activity similar to that of GLP-1R (23, 24). In addition, Phe-345 is close to the binding site of the GCGR antagonist MK-0893 (Fig. 1, *c* and *d*); thus, we hypothesized that Phe-345 is involved in a regulatory element that governs a conformational switch between the active and inactive states of GCGR (Fig. 1). Using AD293 cells expressing exogenous GCGR as our model system (16, 24), we determined cAMP-dependent reporter gene activity as measured for the basal and activated activity of GCGR/G_s signaling in the absence or presence of GCG hormonal peptide. In these experiments, we fused glucagon (residues 1–29) to a long flexible linker and the single membrane-spanning helix of CD8 (25) and co-expressed these chimeric peptides with wild-type (WT) and mutated full-length GCGRs (Fig. 2*a*). Consistent with the previous report (16), in the absence of any ligand, WT GCGR has a very low basal activity, and addition of a membrane-tethered GCG (GCG-M) stimulated an approximately 30-fold increase in cAMP activity (Fig. 2*b*), which was approximately the same level of activation by exogenous GCG at saturated concentration (1 μM GCG in Fig. 2*b*). Thus, we can use the membrane-tethered GCG to mimic saturated concentration of GCG to activate GCGR. Although WT GCGR itself had very low basal activity, substitution of Phe-345 with any of the seven tested hydrophilic amino acids was sufficient to induce significant levels of constitutive G protein-driven cAMP signaling (Fig. 2*c*), whereas only four of eight hydrophobic residue mutations increased cAMP signaling levels (Fig. 2*d*). Interestingly, although the activity of single hydrophilic substitutions at Phe-345 ranged from 2-fold (F345N) to 12-fold (F345K) (Fig. 2*c*, relative basal activity (-fold increase in basal activity of the mutated receptors relative to the basal activity of WT receptor)), surface expression levels for most mutant receptors was well below 40% of WT with the exception of F345S and F345T, which had relative expression levels of 61.0 and 63.8%, respectively (Fig. 2*e*). In contrast, both F345Y and F345C hydrophobic mutations increased receptor surface expression levels without inducing any level of constitutive cAMP signaling (Fig. 2, *d* and *f*). We also noted that for the WT GCGR the basal activity was not dependent upon the surface expression levels or the transfection DNA amounts and remained relatively constant at varying amounts of transfected DNA and surface expression levels (Fig. 2, *g* and *h*). Thus, the constitutive activity of the Phe-345-mutated receptors (*e.g.* F345K) is not due to higher levels of expression but is instead the inherent activation property of these mutated receptors (Fig. 2). Furthermore, the activity of WT or mutated GCGRs can be activated by the membrane-tethered GCG peptide (16) to similar levels, suggesting that mutated receptors were functionally expressed (Fig. 2). To understand why these hydrophilic mutations influence basal cAMP signaling, we examined the antagonist-bound structure of GCGR (Protein Data Bank code 5EE7) (12) and found that Phe-345 is at the center of a hydrophobic interaction network involving three additional residues: Leu-329 and Leu-333 located in TM5 and Met-338 located in ICL3 (Fig. 1, *a* and *b*). In addition, the conformation of TM6 has been shown to be a key determining factor for the receptor to interact with G proteins (17) or arrestin (18) and thus the activation states of the receptor. Interestingly, the GCGR antagonist MK-0893 is bound to a cavity near the Phe-345 position at TM6 (12), resulting in locking the receptor in the inactive conformation (Fig. 1, *c* and d). Thus, we hypothesized that hydrophobic packing mediated by Phe-345 serves as a

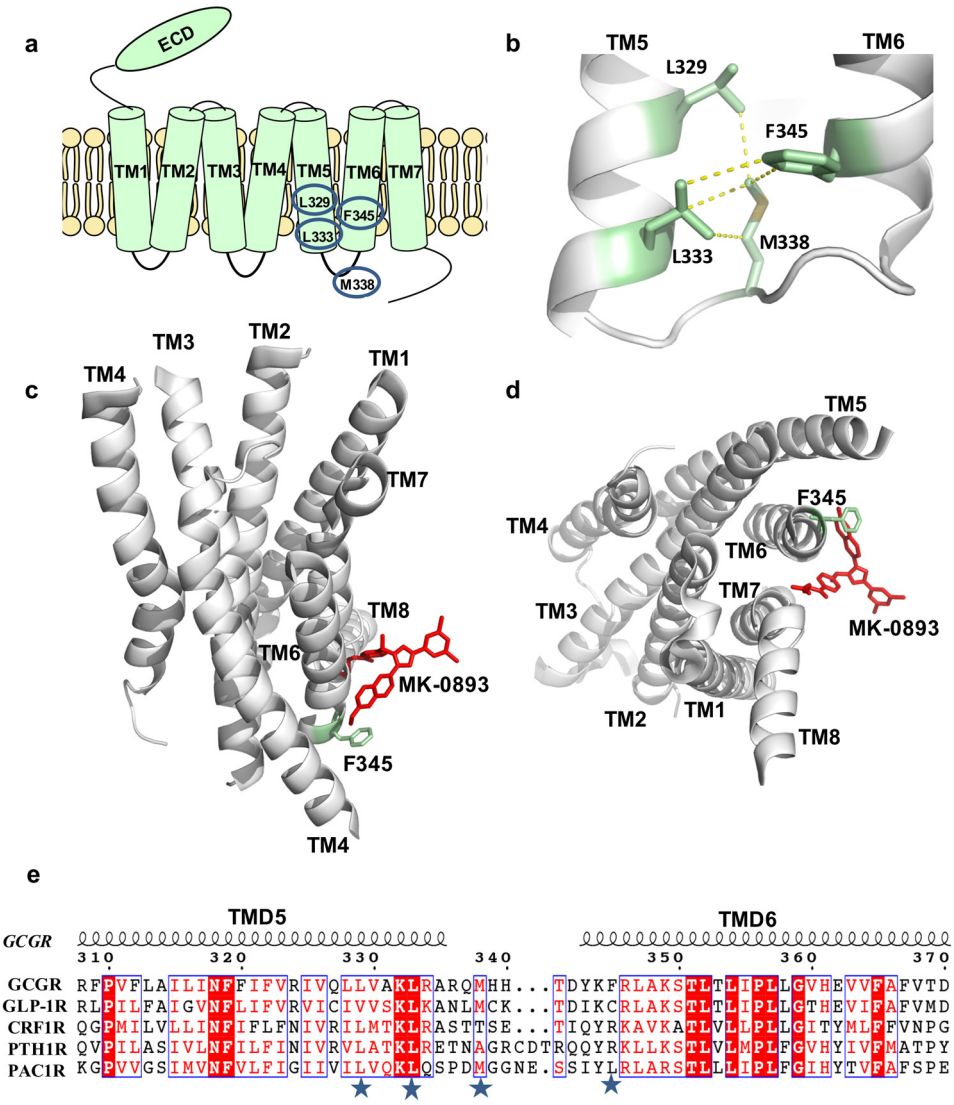

Figure 1. A hydrophobic core comprising Leu-329, Leu-333, Met-338, and Phe-345 in GCGR. *a*, a putative diagram of the human GCGR showing residues that are involved in the hydrophobic patch in this study. The positions of residues Leu-329, Leu-333, Met-338, and Phe-345 are indicated. *b*, close-up of the hydrophobic lock residues Leu-329, Leu-333, Met-338, and Phe-345 in GCGR; the *yellow dashed lines* indicate hydrophobic van der Waals interactions. *c*, the structure of inactive GCCR (Protein Data Bank code 5EE7) is in schematic representation, viewed from the membrane. The MK-0893 antagonist (GCGR antagonist) is shown as a *red stick* model, and Phe-345 is shown as a *green stick* model. *d*, view as in *c* but rotated 90° to view from the cytoplasm. *e*, alignment of partial amino acid sequences of several representative class B GPCRs shows that the hydrophobic lock is only partially conserved. The *blue stars* mark the position of these four hydrophobic amino acids.

hydrophobic lock to keep GCGR in the inactive conformation, and the hydrophilic residue mutations of Phe-345 destabilize this lock, leading to constitutive activation of the receptor as observed above (Fig. 2).

The Phe-345 hydrophobic lock is a dominant regulator of GCGR activity

To assess the contribution of each residue to this newly identified hydrophobic lock, we performed additional mutagenesis screens on Leu-329, Leu-333, and Met-338 similar to that of Phe-345. As expected, when Met-338 was mutated to any of the four polar residues tested (M338E/D/R/K), basal cAMP signaling increased significantly (7–11-fold higher than the WT; Fig. 3*a*) despite a significant reduction in cellular surface expression ($\sim<$ 40% of WT; Fig. 3*c*). Of the hydrophobic residues screened, M338P/F/A and to a lesser extent M338V substitutions were able to significantly increase basal cAMP signaling (Fig. 3*b*) and similarly reduced expression levels (Fig. 3*d*). In contrast, the M338L and M338I mutants did not show any constitutive activity even though they have increased expression levels (Fig. 3, *b* and *d*). Combination of both M338K and F345K mutations (F345K,M338K) further increased the basal cAMP signaling to a level greater than that of any single point mutants tested (F345K or M338K; Figs. 2*c* and 3*a*). In contrast to Met-338 and Phe-345, most residue substitutions at Leu-329 and Leu-333 from TM5 were not able to induce the same levels of cAMP signaling as mutations at residues Met-338 and Phe-345 (Fig. 4). Although L333R, L333D, and L333E mutated receptors had higher expression levels than WT, L333R and L333D did not increase basal and GCG-induced activation, and L333E only induced relatively small increases (1.5-fold) of basal activity. Notably, receptors with L333P, L329P, and L329G

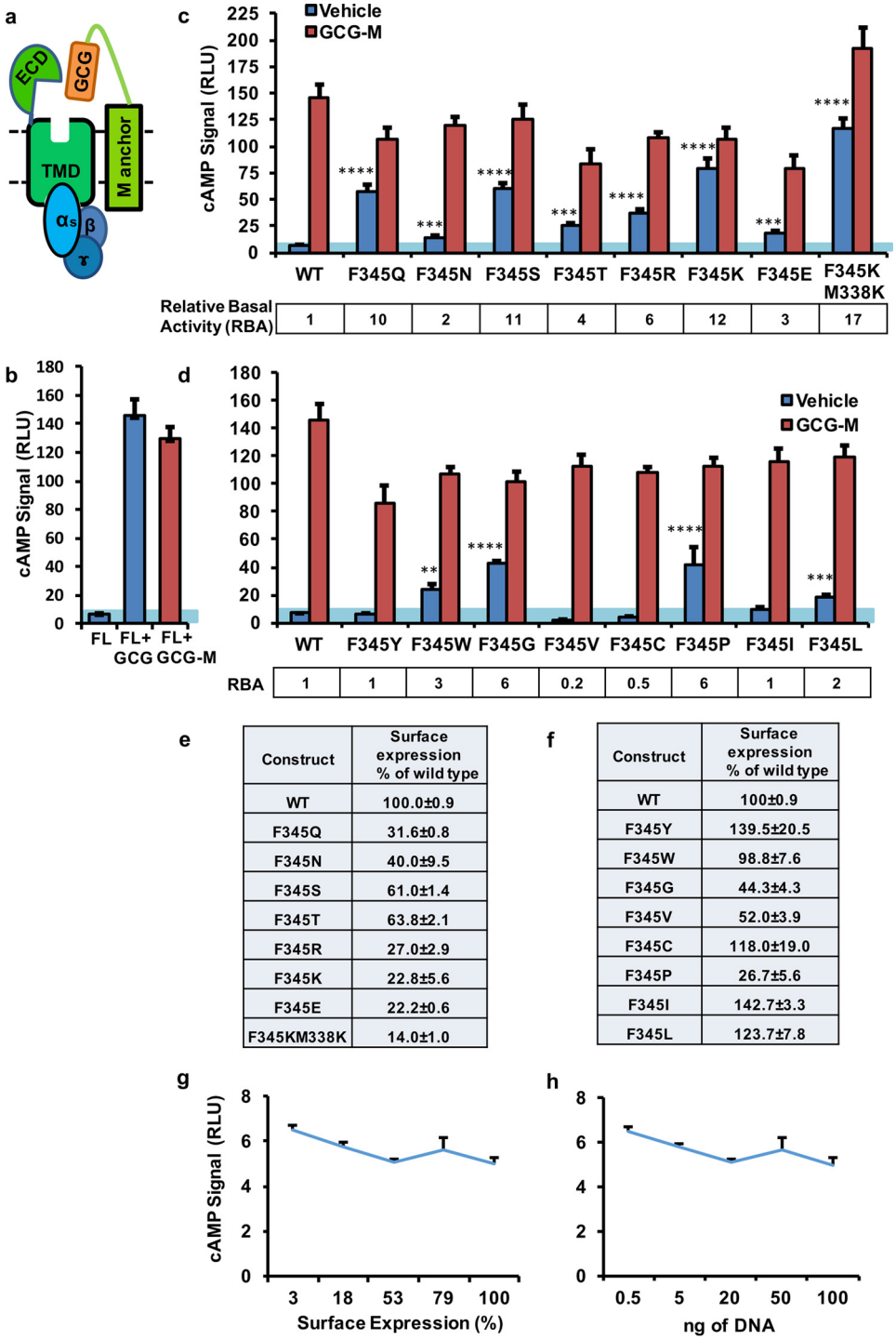

Construct	Surface expression % of wild type
WT	100.0±0.9
F345Q	31.6±0.8
F345N	40.0±9.5
F345S	61.0±1.4
F345T	63.8±2.1
F345R	27.0±2.9
F345K	22.8±5.6
F345E	22.2±0.6
F345KM338K	14.0±1.0

Construct	Surface expression % of wild type
WT	100±0.9
F345Y	139.5±20.5
F345W	98.8±7.6
F345G	44.3±4.3
F345V	52.0±3.9
F345C	118.0±19.0
F345P	26.7±5.6
F345I	142.7±3.3
F345L	123.7±7.8

Figure 2. cAMP signaling and cell surface expression of the Phe-345-mutated GCGR. *a*, schematic presentation of G protein activation by the full-length GCGR when co-expressed with membrane-tethered GCG. *b*, comparison of cAMP signaling of WT GCGR induced by 1.0 μM exogenous GCG and GCG-M. *c* and *d*, basal and membrane-tethered GCG-stimulated cAMP signaling by WT and Phe-345-mutated GCGR with hydrophilic residues (*c*) or hydrophobic residues (*d*). The *blue background* indicates the basal activity of WT full-length GCGR. Relative basal activity (*RBA*), -fold increase in basal activity of the mutated receptors relative to the WT. *Error bars* represent S.D. of triplicate determinations. Two-tailed Student's *t* test was used to determine *p* values for data point *versus* wild-type basal activity: **, $p \leq 0.01$; ***, $p \leq 0.001$; ****, $p \leq 0.0001$. *e* and *f*, cell surface expression of WT and Phe-345-mutated GCGR with hydrophilic amino acids (*e*) and hydrophobic residues (*f*). Data are presented as percentage of the WT GCGR expression level. *g* and *h*, correlation of cAMP signal with surface expression levels of GCGR (*g*) and amounts of transfected DNA (*h*). Note that the cAMP signal is relatively constant at varying amounts of transfected DNA and surface expression levels. *RLU*, relative luciferase unit, which is the ratio of the CRE-luciferase activity to the *Renilla luciferase* activity.

mutations had sufficient levels of cell surface expression (>25% of WT GCGR), but they failed to respond to GCG stimulation, indicating that these mutated receptors are most likely non-functional because Leu-329 and Leu-333 are located at the end of TM5, and its helical conformation is easily broken by Pro and Gly mutations. In addition, struc-

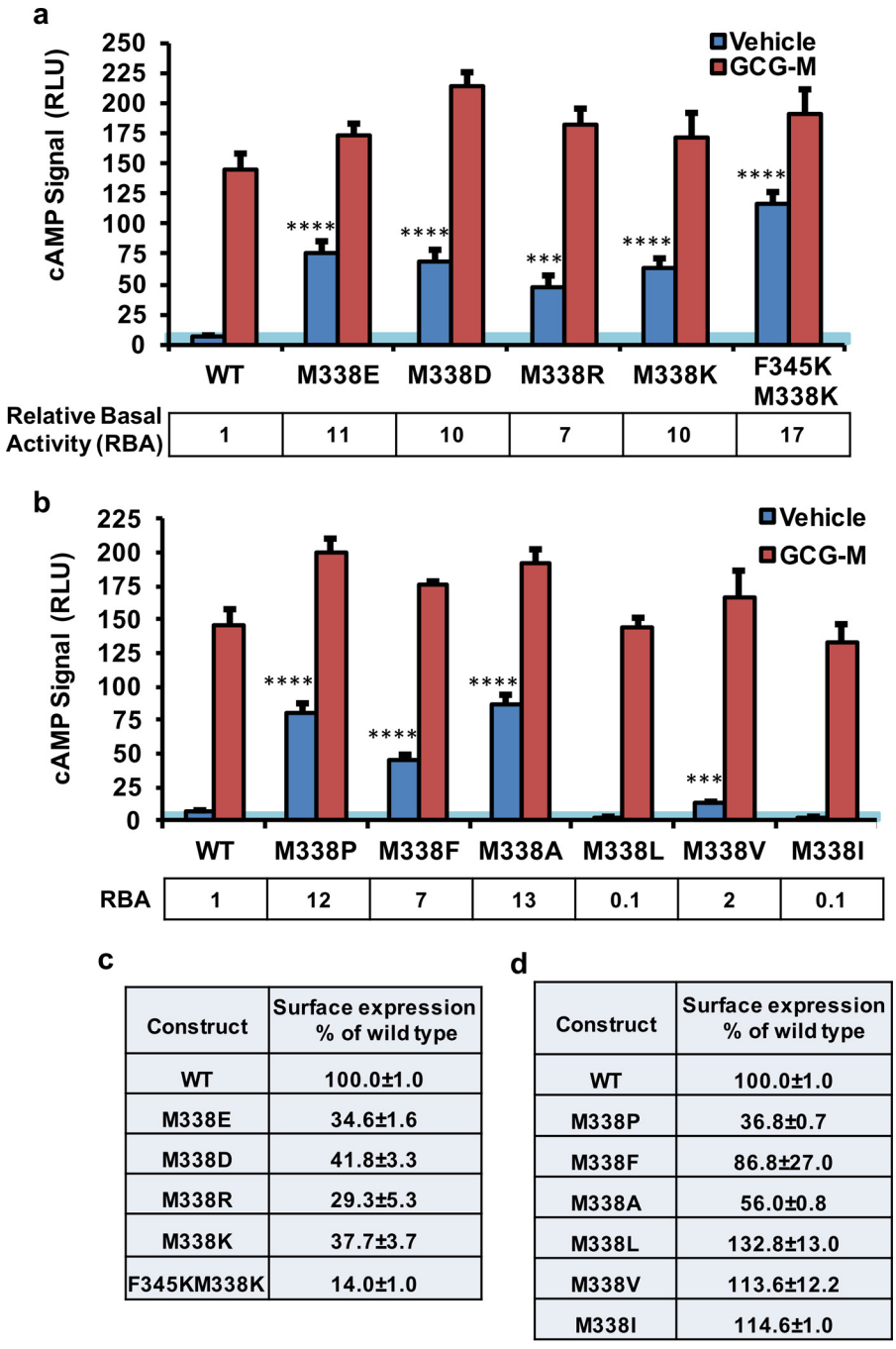

c

Construct	Surface expression % of wild type
WT	100.0±1.0
M338E	34.6±1.6
M338D	41.8±3.3
M338R	29.3±5.3
M338K	37.7±3.7
F345KM338K	14.0±1.0

d

Construct	Surface expression % of wild type
WT	100.0±1.0
M338P	36.8±0.7
M338F	86.8±27.0
M338A	56.0±0.8
M338L	132.8±13.0
M338V	113.6±12.2
M338I	114.6±1.0

Figure 3. cAMP signaling and cell surface expression of Met-338-mutated GCGR. *a* and *b*, basal and membrane-tethered GCG-stimulated cAMP signaling of WT and Met-338-mutated GCGR with hydrophilic amino acids (*a*) and hydrophobic amino acids (*b*). The *blue bars* represent the basal activity, and *red bars* represent the activity stimulated by membrane-tethered GCG. The *blue background* indicates the basal activity of WT full-length GCGR. Relative basal activity (*RBA*), -fold increase in basal activity of the mutated receptors relative to the WT. *Error bars* represent S.D. of triplicate determinations. Two-tailed Student's *t* test was used to determine *p* values for data point *versus* wild-type basal activity: ***, $p \leq 0.001$; ****, $p \leq 0.0001$. *c* and *d*, cell surface expression of GCGR mutated with hydrophilic amino acids (*c*) and hydrophobic amino acids (*d*) at position Met-338. Data are presented as percent expression level relative to that of the WT receptor (100%). *RLU*, relative luciferase unit, which is the ratio of the CRE-luciferase activity to the *Renilla* luciferase activity.

tural comparison of active and inactive GPCR pairs, including β2AR (17) and rhodopsin (18), reveals that the major conformational changes are in the TM6 positions (see later in Fig. 8*a*), whereas the TM5 positions move very little, which may explain why mutations at Leu-329 and Leu-333 from TM5 have less effect on the basal activation of the receptor than the mutations at TM6.

For full-length GCGR, the ECD has been shown to be required for receptor activation in addition to its activity in ligand binding (16), and a putative ECD-TMD interaction was proposed as one of the major forces to keep the receptor in an inactive conformation (14, 15, 26). To probe the relationship between the hydrophobic lock and the ECD, we introduced the ECL3 mutation, which replaces the ECL3 of GCGR with ECL3

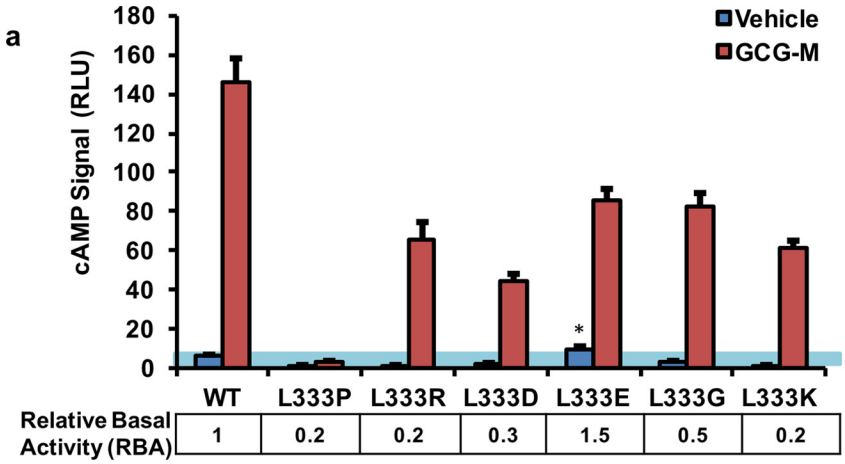

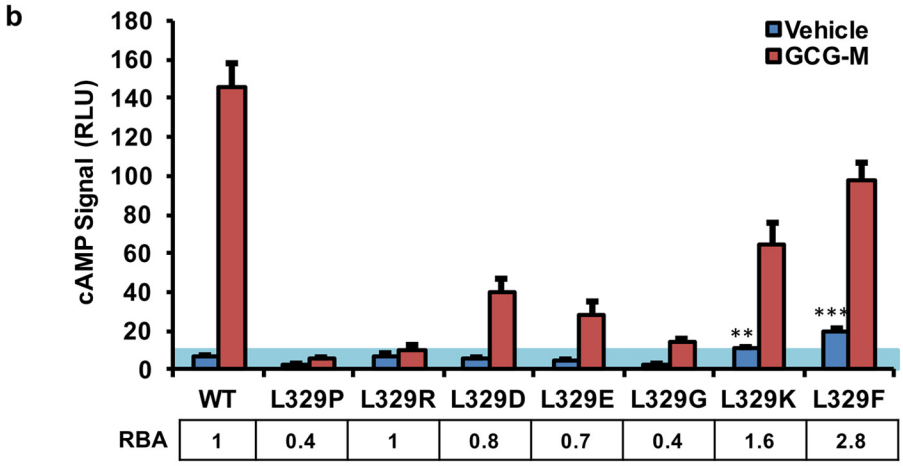

c

Construct	Surface expression % of wild type
WT	100.0±1.0
L333P	33.5±1.6
L333R	167.1±2.3
L333D	145.7±1.9
L333E	119.4±3.5
L333G	75.3±4.2
L333K	64.7±1.7

d

Construct	Surface expression % of wild type
WT	100
L329P	28.5±2.6
L329R	36.9±1.8
L329D	28.5±2.6
L329E	18.7±2.6
L329G	48.8±3.7
L329K	20.9±1.9
L329F	23.6±1.5

Figure 4. cAMP signaling and cell surface expression of GCGR with mutations at positions Leu-329 and Leu-333 located at TM5. *a* and *b*, the basal and membrane-tethered GCG peptide-stimulated cAMP signaling of GCGR with mutations introduced at position Leu-329 (*a*) and Leu-333 (*b*). The *blue bars* represent the basal activity, and *red bars* represent the activity stimulated by membrane-tethered GCG. Relative basal activity (*RBA*), -fold increase in basal activity of the mutated receptors relative to the WT receptor. The *blue background* indicates basal activity of the wild-type full-length GCGR. *Error bars* represent S.D. of triplicate determinations. Two-tailed Student's *t* test was used to determine *p* values for data point *versus* wild-type basal activity: *, $p \leq 0.05$; **, $p \leq 0.01$; ***, $p \leq 0.001$. *c* and *d*, cell surface expression of GCGR with amino acid substitutions at positions Leu-329 (*c*) and Leu-333 (*d*) are shown. Data are presented as percentage of the WT GCGR expression level (100%). *RLU*, relative luciferase unit, which is the ratio of the CRE-luciferase activity to the *Renilla* luciferase activity.

of GLP-1R, and another mutation, Y65A, to GCGR (Fig. 5*a*, ECL3 and Y65A). Both of these mutations were reported to decouple ECD inhibition of its TMD to promote constitutive cAMP signaling (15). However, as shown in Fig. 5 (ECL3 and Y65A), their basal activities were similar to that of the WT receptor in our assay system, which is much lower than the basal activation induced by mutations in the hydrophobic lock, suggesting that the hydrophobic lock we identified here is the dominant regulator of GCGR activity compared with the ECD-TMD interaction. Furthermore, we expressed ECD-truncated receptors containing the Met-338 or Phe-345 mutation and quantified their cAMP signaling levels (Fig. 5*a*). WT GCGR

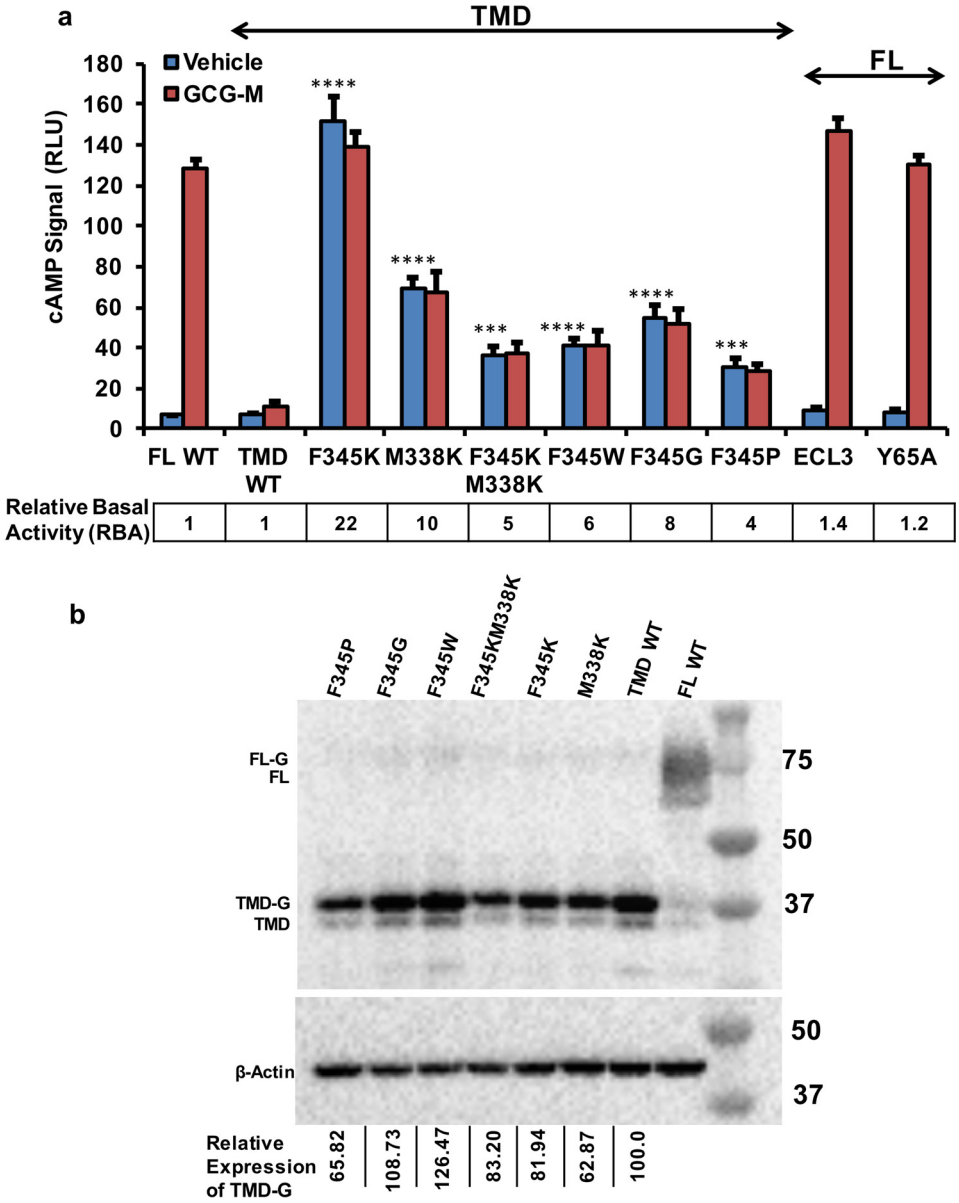

Figure 5. Role of the ECD in the constitutive activation of mutated GCGR. *a*, cAMP signal of the GCGR TMD with mutations in hydrophobic lock residues (F345K; M338K; and F345K,M338K) or in TM6 Phe-345 (F345W, F345G, and F345P) and of full-length GCGR with mutations in ECL3 and Tyr-65. Relative basal activity (*RBA*), -fold increase in basal activity of the mutated receptors relative to the WT receptor. *Error bars* represent S.D. of triplicate determinations. Two-tailed Student's *t* test was used to determine *p* values for data point *versus* the basal activity of the WT TMD: ***, $p \leq 0.001$; ****, $p \leq 0.0001$. *b*, Western blot analysis of WT GCGR TMD or TMD with constitutively activating mutations. All immunoblottings were performed with anti-FLAG antibody for detection and anti-β-actin antibody for normalization. Each lane was normalized by β-actin. Relative expression was calculated from the glycosylated band (*TMD-G*), which roughly represents the surface expression of TMDs, with expression of wild-type TMD as 1.00. *FL*, full-length; *FL-G*, glycosylated full-length WT GCGR. *RLU*, relative luciferase unit, which is the ratio of the CRE-luciferase activity to the *Renilla* luciferase activity.

TMD showed low basal activity that was not further activated by addition of the membrane-tethered GCG (Fig. 5*a*, TMD WT). In contrast, all TMD mutants exhibited varying degrees of constitutive activities with the F345K mutant having the highest basal activity, which was even higher than that of full-length WT receptor activated by GCG (Fig. 5*a*). Co-transfection with the membrane-tethered GCG hormonal peptide did not further increase the cAMP signaling levels of the mutated receptors. Western blot analysis indicated that the surface expression levels of all these mutated TMDs were similar to that of the WT GCGR TMD (Fig. 5*b*, *Relative Expression of TMD-G*). Taken together, these results suggest that mutations at residues Met-338 and Phe-345 can induce the receptor TMD activation regardless of the presence of the receptor ECD.

Constitutive G protein mutants led to constitutive arrestin recruiting activity

Next we sought to evaluate whether the mutations in Met-338 or Phe-345 that cause constitutive G protein signaling could also result in β-arrestin1 recruitment to GCGR (27). To quantify interaction between GCGR and β-arrestin1, we adopted a previously developed Tango assay (18) in which the C-terminal tail of GCGR is fused with a tobacco etch virus (TEV) protease cleavage site and the transcriptional activator

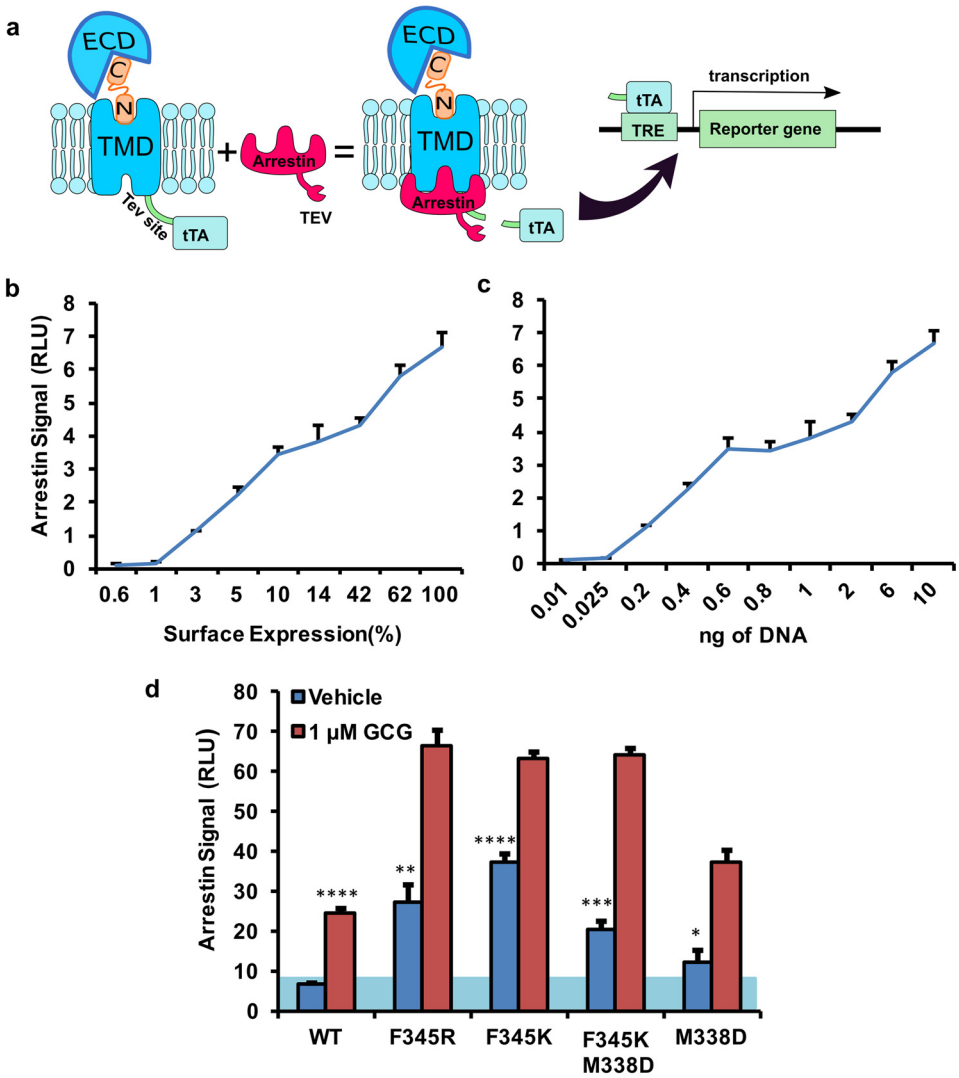

RBA	1	4.1	5.6	3.1	1.9
Plasmid Increased Fold	1X	3.8X	4.4X	7.2X	2.4X
Surf. Expression % of W T	100	40.3	47.6	30.4	54.9

Figure 6. Mutations that constitutively activate G protein signaling also induced constitutive arrestin recruitment. *a*, diagram of the Tango assay to detect arrestin binding through luciferase reporter signals. tTA/transcriptional response element (*TRE*)-luciferase reporter signals serve as a measure for β-arrestin1 recruitment by WT and mutant receptors. *b* and *c*, correlation of arrestin recruitment signals with surface expression levels of WT GCGR (*b*) and with amounts of transfected DNA (*c*). Note that the arrestin recruitment signals change along with the increasing amounts of transfected DNA and the levels of surface-expressed WT GCGR. *d*, basal and exogenous GCG-stimulated arrestin signals by mutant receptors that can constitutively activate the G protein signaling pathway. *Plasmid Increased Fold*, -fold increase in the amount of transfected DNA based on the difference of surface expression between wild-type and mutant GCGR (see Figs. 2*c* and 3*c*). Relative basal activity (*RBA*), -fold increase in basal activity of the mutated receptors relative to the WT receptor. *Surf. Expression % of WT*, relative surface expression of constructs at the indicated -fold amount of transfected DNA. The *blue background* indicates basal activity of wild-type full-length GCGR. *Error bars* represent S.D. of triplicate determinations. Two-tailed Student's *t* test was used to determine *p* values for data point *versus* the basal activity of the WT GCGR: *, $p \leq 0.05$; **, $p \leq 0.01$; ***, $p \leq 0.001$; ****, $p \leq 0.0001$. *RLU*, relative luciferase unit, which is the ratio of the CRE-luciferase activity to the *Renilla* luciferase activity.

tTA, whereas β-arrestin1 is fused with TEV protease at its C terminus. Recruitment of β-arrestin1 to the activated GCGR leads to cleavage at its TEV site and release of tTA to induce expression of the luciferase reporter (Fig. 6*a*). In contrast to G protein-mediated signaling, the arrestin recruitment signal we detected was highly dependent on receptor surface expression levels as the arrestin recruiting signal of WT GCGR increased along with the increase of the surface expression and the amount of transfected DNA (Fig. 6, *b* and *c*). As shown in Fig. 6*d*, WT GCGR has a basal arrestin recruitment signal, and addition of a saturated amount of GCG (1 μM) induced 4-fold higher signal (Fig. 6*d*). Because the constitutively active receptors had lower expression levels (Figs. 2*e* and 3*c*), which affect arrestin recruitment signaling, we increased the amount of transfected DNA for the constitutively active receptor expression constructs (F345R; F345K; F345K,M338D; and M338D mutated

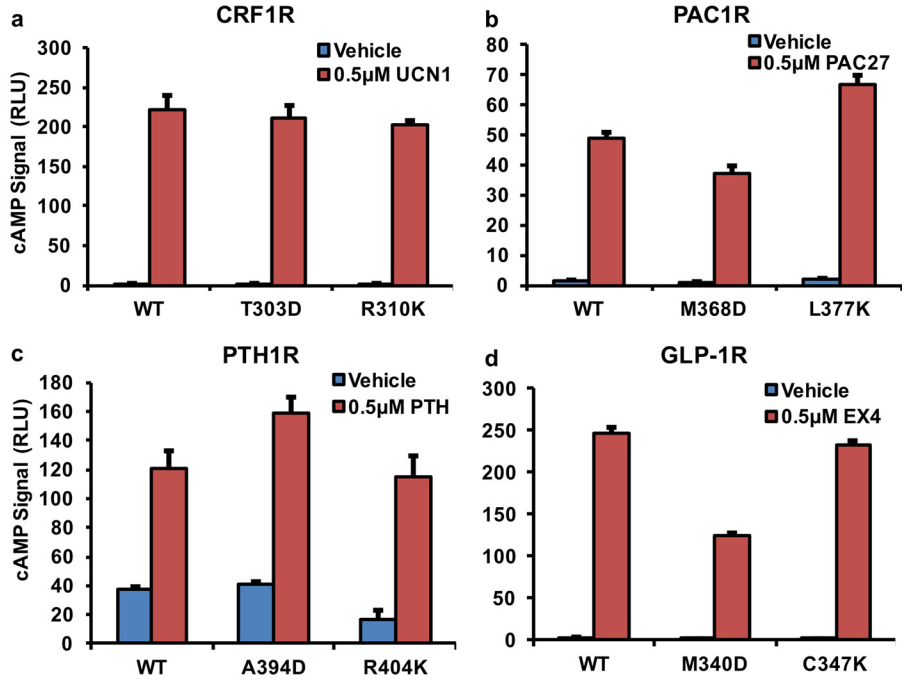

Figure 7. Function of the GCGR hydrophobic lock is not conserved in other class B GPCRs. Basal (*blue bars*) and ligand-activated (*red bars*) cAMP signals of the WT and mutant receptors CRF1R (*a*), PAC1R (*b*), PTH1R (*c*), and GLP-1R (*d*) are shown. The mutations in different receptors correspond to M338D and F347K in GCGR. All ligands were used at saturated levels that were saturated for activation of their cognate receptors. *Error bars* represent S.D. of triplicate determinations. *RLU*, relative luciferase unit, which is the ratio of the CRE-luciferase activity to the *Renilla* luciferase activity. *PTH*, parathyroid hormone; *EX4*, exendin-4.

receptors) by 2.4–7.2-fold (Fig. 6*d*, *Plasmid Increased Fold*) to increase their surface expression. Even with the increased amount of transferred DNAs, the expression levels of the Met-338 and Phe-345 mutants were only 30.4–54.9% of the WT receptors (Fig. 6*d*, *Surf. Expression % of WT*). The arrestin recruitment signals, regardless of the absence or presence of 1 μM GCG, were significantly higher than that of the WT receptor (Fig. 6*d*), indicating that these mutated receptors can also cause constitutive arrestin recruitment activity.

Disruption of a conserved polar core leads to constitutive activation of several class B GPCRs

Sequence alignment of the Phe-345 hydrophobic lock indicates that Met-338 and Phe-345 are not conserved in other members of class B GPCRs (Fig. 1*d*). Consistently, the corresponding mutations of Met-338 and Phe-345 positions in CRF1R, PAC1R, PTH1R, and GLP-1R did not induce any constitutive activity (Fig. 7), suggesting that the hydrophobic lock mechanism might only be specific to the GCGR but not applicable to other members of class B GPCRs. To seek a broader mechanism of class B GPCR activation, we performed a structural alignment of the activated β_2AR bound to the G protein complex (Protein Data Bank code 3SN6) (17), activated rhodopsin in complex with arrestin (Protein Data Bank code 4ZWJ) (18), and GCGR (Protein Data Bank code 5EE7) (12) in its inhibited conformation (Fig. 8). Comparison of these three receptor states reveals that the most pronounced change is the outward swing of TM6 with residue Thr-351 serving as a pivotal point (Fig. 8, *a* and *b*). Inspection of the inactive GCGR structure reveals that Thr-351 forms a hydrogen bond with Tyr-400 from TM7 (Fig. 8, *c* and *d*). In addition, Tyr-400 from TM7 forms a stacking interaction with His-177 from TM2, which itself forms a hydrogen bond with Glu-245 from TM3 (Fig. 8, *c* and *d*). Sequence analyses indicate that all four residues are 100% conserved in class B GPCRs (Fig. 8, *e*–*h*), suggesting that these four residues form a conserved polar core within the bottom of the TMD bundle. Importantly, His-223 and Thr-410 of PTH1R, analogous to His-177 and Thr-351 of GCGR, respectively, were previously identified as mutational hot spots in patients with Jansen's metaphyseal chondrodysplasia arising from constitutive ligand-independent PTH1R activation (29, 30). In addition, we found that the corresponding Thr-351 residue is conserved in rhodopsin (Thr-251) and β_2AR (Thr-274) and is located at the same critical pivotal point of the TM6 hinge (Fig. 8*b*). Together, these observations led us to hypothesize that the conserved Thr-351 polar core plays a critical role in receptor activation by locking TM6 in the inactive conformation.

To test the role of Thr-351 in GCGR activation, we performed a mutational screening similar to that of Phe-345 and assessed differential cAMP signaling levels and arrestin recruiting activities. Consistent with previously reported mutational screening at the corresponding residue in PTH1R, Thr-410, most amino acid substitutions at Thr-351 in GCGR were sufficient to induce robust levels of ligand-independent cAMP signaling ranging from 34-fold (T351M) to 2-fold (T351Q) above the basal level of the WT receptor without comprising the GCG-stimulated signal (Fig. 8*a*) despite significant reductions in surface expression levels (Fig. 9*b*), suggesting that threonine at this position functions to constrain the receptor in the inactive conformation. Basal cAMP signaling of cells expressing mutant receptors (Met, Val, Cys, Ile, and Ala) reached up to 100–160% of the levels obtained with WT GCGR that had been

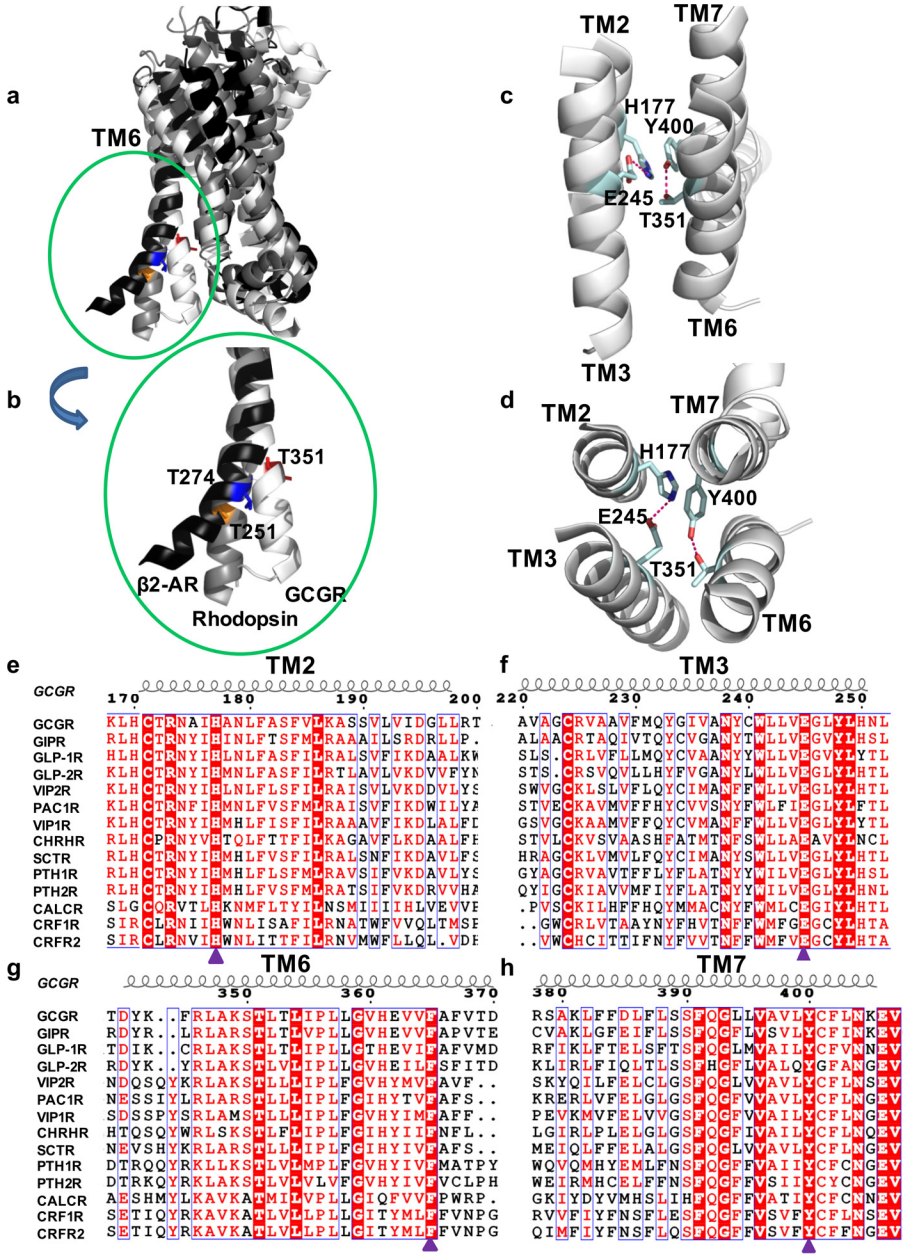

Figure 8. A conserved polar core formed by residues from TM2, TM3, TM6, and TM7 of class B GPCRs. *a*, structure superposition of rhodopsin in active and arrestin-bound conformation (*gray*; Protein Data Bank code 4ZWJ), β_2AR in active and G_s-bound conformation (*black*; Protein Data Bank code 3SN6), and GCGR in inactive conformation (*white*; Protein Data Bank code 5EE7). Arrestin, G_s, and fusion protein were omitted for clarity. *b*, superposition of TM6 of rhodopsin, β_2AR, and GCGR. The conserved GCGR residue Thr-351 at the pivot point of TM6 is shown in *red stick* representation, and the corresponding residues rhodopsin Thr-251and β_2AR Thr-274 are shown in *orange* and *blue stick* representations, respectively. *c* and *d*, two 90° views of the GCGR polar core structure. Extracellular and intracellular loops have been removed for clarity. The polar core residues His-177 at TM2, Glu-245 at TM3, Thr-351 at TM6, and Tyr-400 at TM7 are labeled in *blue stick*. The *red dashed lines* indicate hydrogen bonding between polar core residues. *e–h*, sequence alignment of the polar core helices of class B GPCRs: TM2 (*e*), TM3 (*f*), TM6 (*g*), and TM7 (*h*). *Purple triangles*, conserved polar core residues. *CALCR*, calcitonin receptor; *SCTR*, secretin receptor; *GIPR*, gastric inhibitory polypeptide receptor; *GHRHR*, growth hormone-releasing hormone receptor.

stimulated with membrane-tethered GCG peptide, indicating that these mutated receptors can achieve full activation of the G protein signaling in a ligand-independent manner. An interesting phenomenon was that the positive charged residue mutations (T351R and T351K) can produce constitutive activation and preserve GCG-M responsiveness despite very low membrane expression (4.9 and 8.6% of WT, respectively), whereas negative charge mutations (T351E and T351D) not only failed to cause constitutive activation but also eliminated the response to GCG-M despite better levels of expression (22 and 14% of WT, respectively) (Fig. 9*a*). Based on further inspection of the inactive GCCR structure (12) (Protein Data Bank code 5EE7), T351D/E could act as a hydrogen bond acceptor to the hydroxyl group on Tyr-400, locking the receptor in an inactive conformation. In addition, T351D/E mutation could cause charge repulsion with another polar core residue, Glu-245, which could destabilize the polar core and result in a nonfunctional receptor that cannot be activated by the tethered GCG. In contrast, T351R/K could act as a hydrogen bond donor (or participate in cation-π interaction in the case of T351K) to

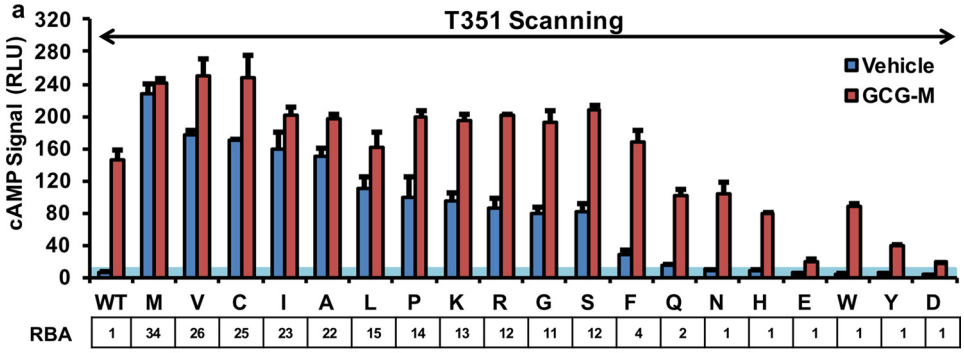

b

Construct	Surface expression % of wild type
WT	100.0±1.0
T351M	26.9±0.8
T351V	19.4±1.2
T351C	12.0±0.9
T351I	15.9±2.3
T351A	32.3±2.0
T351L	29.2±3.0
T351P	4.8±1.8
T351K	4.9±1.9
T351R	8.6±0.9
T351G	47.9±0.9
T351S	42.6±1.3
T351F	69.6±1.8
T351Q	22.5±2.0
T351N	28.3±1.3
T351H	46.5±2.1
T351E	22.1±0.8
T351W	48.8±1.4
T351Y	55.5±1.9
T351D	14.4±0.6

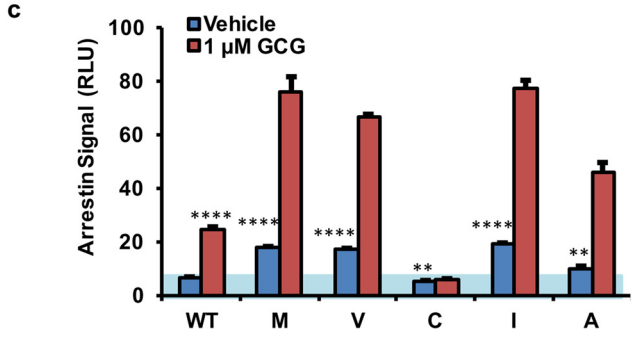

	WT	M	V	C	I	A
RBA	1.0	2.6	2.5	0.8	2.8	1.5
Plasmid Increased Fold	1X	5X	5X	9X	6X	3X
Surf Expression % of W T	100	71.3	70.2	30.5	67.8	80.2

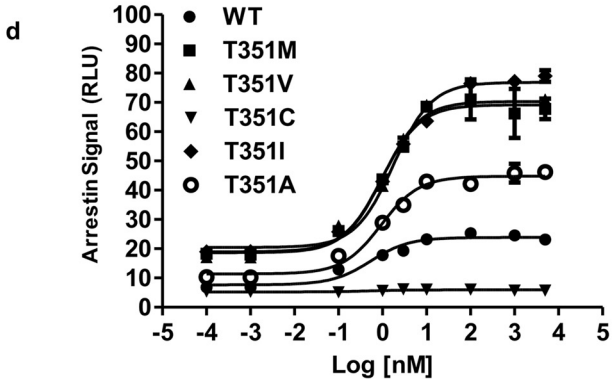

Figure 9. Effect of Thr-351 mutations on GCGR activity and expression. *a*, basal and GCG-stimulated cAMP accumulation by full-length WT and Thr-351-mutated GCGR, rearranged by the strength of the basal cAMP signal (from *right* to *left*). The *blue background* indicates the basal activity of full-length WT GCGR. Relative basal activity (*RBA*), -fold increase in basal activity of the mutated receptors relative to the WT receptor. *Error bars* represent S.D. of triplicate determinations. *b*, cell surface expression of full-length GCGR with amino acid substitutions at position Thr-351. Data are presented as percent expression levels relative to that of WT receptor. *c*, arrestin signal by mutant GCGRs that produces high basal G protein signal. *Plasmid Increase Fold*, -fold increase in the amount of transfected DNA based on the difference of surface expression between wild type and mutations (see Fig. 8*b*). Relative basal activity (*RBA*), -fold increase in basal activity of the mutated receptors relative to the WT receptor. *Surf. Expression % of WT*, relative surface expression of constructs at the indicated -fold amount of transfected DNA. The *blue background* marks the basal activity of full-length WT GCGR. *Error bars* represent S.D. of triplicate determinations. Two-tailed Student's *t* test was used to determine *p* values for data point *versus* the basal activity of the WT GCG receptor: **, $p \leq 0.01$; ****, $p \leq 0.0001$. *d*, dose-dependent arrestin recruitment signals by mutant receptors. All values are means ± S.E. (*error bars*) of two independent experiments, each conducted in triplicate. *RLU*, relative luciferase unit, which is the ratio of the CRE-luciferase activity to the *Renilla* luciferase activity.

the tyrosine hydroxyl, but because the side chain length of Lys/Arg is much longer than Asp/Glu, the interaction would require TM6 to be pushed out toward an active conformation. Thus, T351R/K instead of T351D/E mutated receptors tend to be more constitutively active.

In arrestin recruitment assays, we chose the top five mutations (Met, Val, Cys, Ile, and Ala) that induced the highest constitutive G protein signal (Fig. 9*a*) and introduced them to the Tango system. Considering that the arrestin recruiting capacity of the receptor is highly correlated with its surface expression levels (Fig. 6, *b* and *c*) and that these mutated receptors showed dramatic decreases in their surface expression (Fig. 9*b*; 12.0–32.3% of WT), we increased the transfected plasmid DNA 3–9-fold relative to the WT receptor to increase their surface expression (Fig. 9, *c* and *d*). Except for the T351C mutant, all these mutated receptors constitutively activated the arrestin

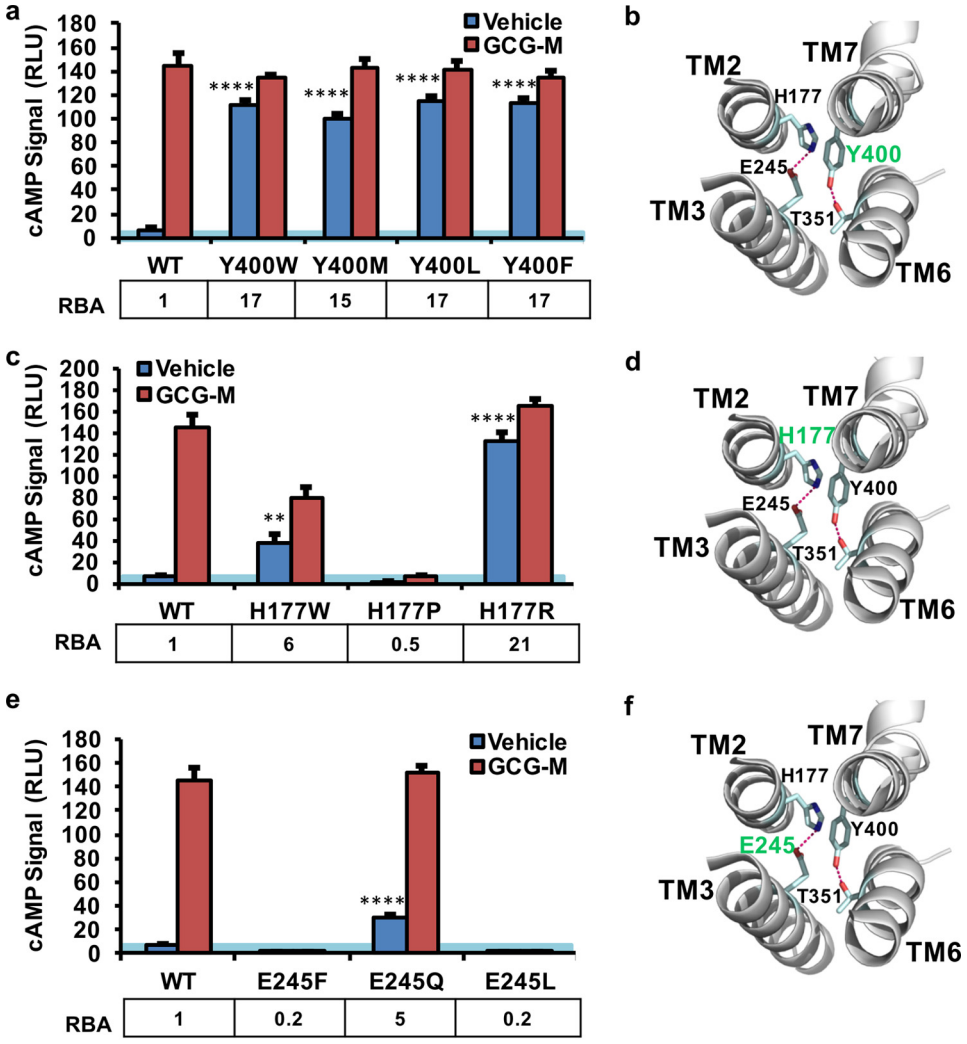

g

Construct	Surface expression % of wild type	Construct	Surface expression % of wild type	Construct	Surface expression % of wild type
Y400W	30.9±0.8	H177W	20.9±0.4	E245F	0.5±0.2
Y400M	23.8±0.1	H177P	1.6±0.6	E245Q	26.9±0.5
Y400L	23.0±0.3	H177R	13.9±0.1	E245L	0.6±0.1

Figure 10. Polar core mutations increase basal GCGR activity. *a*, *c*, and *e*, basal and membrane-tethered GCG-stimulated cAMP signals of GCGR with mutations at position Tyr-400 (*a*), His-177 (*c*), and Glu-245 (*e*). The *blue background* marks the basal activity of the wild-type full-length GCGR. Relative basal activity (*RBA*), -fold increase in basal activity of mutant receptors relative to WT receptor. *Error bars* represent S.D. of triplicate determinations. Two-tailed Student's *t* test was used to determine *p* values for data point *versus* the basal activity of WT GCGR: **, $p \leq 0.01$; ****, $p \leq 0.0001$. *b*, *d*, and *f*, structure of the GCGR polar core in which residues Tyr-400 (*b*), His-177 (*d*), and Glu-245 (*f*) are highlighted in *green*. *g*, cell surface expression of GCGR with substitutions at position Tyr-400, His-177, and Glu-245. Data are presented as percent expression levels relative to that of WT receptor (100%). *RLU*, relative luciferase unit, which is the ratio of the CRE-luciferase activity to the *Renilla* luciferase activity.

recruitment signal, which was further promoted by addition of GCG (Fig. 9, *c* and *d*). Quantitative analysis showed that the expression levels of these mutant GCGRs were still lower than that of the WT receptor even though the amounts of transferred DNA were increased (Fig. 9*c*), suggesting that receptor activity negatively correlates with expression. It was interesting to note that the T351C mutation transforms the receptor into a constitutive G protein-biased receptor, which only activates the G protein signal pathway (Fig. 9*a*), but was not able to activate arrestin signaling (Fig. 9, *c* and *d*) even in the presence of a saturated amount of GCG peptide ligand (Fig. 9*d*).

In the inactive GCGR structure, Thr-351 forms a close hydrogen bond with Tyr-400 from TM7 (Fig. 10*b*). The high level of constitutive activity induced by the T351V mutation indicates that the hydrogen bond between Thr-351 and Tyr-400 is critical to the TM6 locking mechanism because the only

difference between Thr-351 and T351V is a hydroxyl (-OH) group in the side chain in Thr-351 *versus* a methyl group in T351V. To corroborate this observation, we made the Y400F mutation, which removes the hydroxyl group from tyrosine, and found that the Y400F mutated receptor was constitutively active (Fig. 10*a*). Several other Tyr-400 mutations, including Y400W, Y400M, and Y400L, which were predicted not to form the hydrogen bond with Thr-351, all resulted in constitutive activation of the mutated receptors (Fig. 10*a*). We also mutated the other two residues, His-177 and Glu-245, of the polar core. For His-177, which is analogous to His-223 in PTH1R that was previously identified as a mutational hot spot in patients with Jansen's metaphyseal chondrodysplasia arising from constitutive ligand-independent PTH1R activation (29, 30), H177W and H177R mutations could induce ligand-independent activity for GCGR (Fig. 10, *c* and *d*). For residue Glu-245, the E245Q mutation increased basal activity by 5-fold higher relative to the WT receptor, whereas the E245F and E245L (as well as H177P) mutations seemed to produce non-functional receptors that were not activated by membrane-tethered GCG and that have very poor expression (Fig. 10, *c*, *e*, and *g*). As expected, the surface expression of all these mutations decreased dramatically (Fig. 10*g*). Collectively, the above data suggest that the packing interactions and hydrogen bonds of the polar core are essential to keep GCGR in the inactive state, and mutations that alter this polar core result in either non-functional receptors or constitutively active receptors.

We next sought to determine whether the polar core mechanism is conserved in other members of class B GPCRs. To address this, we mutated the corresponding polar core in five additional members of class B GPCRs: PAC1R, VIP1R, CRF1R, PTH1R, and GLP-1R. As shown in Fig. 11, most mutations of the polar core residues in PAC1R (Fig. 11, *a* and *b*), VIP1R (Fig. 11, *c* and *d*), and PTH1R (Fig. 11*g*) resulted in constitutively active receptors. Although several mutations in residues Thr-316 and His-155 of CRF1R did not alter the basal activity of the receptor, T316V and Y363W mutations did induce significant levels of constitutive activity (Fig. 11, *e* and *f*). In addition, mutations in the GLP-1R polar core resulted in non-functional receptors as these mutated receptors did not respond to the presence of saturated concentration of exendin-4 (Fig. 11*h*). Together, these data suggest that formation of the polar core is indeed a conserved mechanism to stabilize the inactive conformation of class B GPCRs, and mutations that compromise this polar core induce constitutive activity of the receptors or result in non-functional receptors.

Discussion

In this study, we have discovered a common mechanism for activation of class B GPCRs through studying ligand-independent activation of GCGR. Although class B GPCRs are an important family of drug-targeted receptors activated by peptide ligands, the activation mechanism remains largely unknown. This is in great contrast to the much better studied mechanism for activation of class A GPCRs, which revealed an outward swing movement in the cytoplasmic side of TM6 as the hallmark of the receptor activation (17–20, 22). Through comprehensive mutagenesis studies and structural modeling, we have identified a hydrophobic lock and a polar core formed in part by TM6 as the key structural elements that keep TM6 of GCGR in the inactive and closed state. Mutations that disrupt these two structural elements led to constitutive activation of the mutated receptors. Although the hydrophobic lock mechanism is specific to GCGR, the polar core mechanism is conserved in a number of other class B GPCRs that we tested in this study. Together, these results suggest a common activation mechanism of class B GPCRs that involves the outward movement of TM6 on the cytoplasmic side, which is analogous to the activation mechanism of class A GPCRs.

The involvement of TM6 in class B GPCR activation has been supported by a number of previous observations. The first example was the activation of GLP-1R by small molecule electrophiles such as BETP, which modifies Cys-347 near TM6 (23). C347R/K mutations in GLP-1R allow activation of GLP-1R by fusion of a nonspecific 5-residue linker that is devoid of any GLP-1 sequence (24). The hydrophobic lock residue Phe-345 in GCGR is analogous to Cys-347 in GLP-1R. Thus, it is very likely that the activation of GLP-1R by small molecule electrophiles is mediated by destabilization of TM6 from its inactive state. The second example is the constitutive mutations H223R and T410P in PTH1R, which were originally discovered to cause Jansen's metaphyseal chondrodysplasia over 20 years ago (30). Mutations in the homologous GCGR residues also caused constitutive activity (31), and several of these constitutive mutations could be reproduced in our current studies. The basis of these constitutive mutations has remained largely unknown due to the absence of activated class B GPCR structures. Inspection of the recently available inactive GCGR structure (12, 13) reveals that His-177 and Thr-351 form a polar core with Glu-245 from TM3 and Tyr-400 from TM7. Mutations in Glu-245 and Tyr-400 can also cause constitutive activity of GCGR, suggesting that this polar core is a key structural element that holds TM6 of GCGR in the inactive conformation (Fig. 10). Notably, these four residues that comprise the polar core are 100% conserved in all class B GPCRs, and their corresponding mutations in PAC1R, VIP1R, CRF1R, and PTH1R also resulted in constitutive activity of the receptors, suggesting that the polar core is a conserved structural feature to keep class B GPCRs in the inactive state in the absence of their peptide agonists.

The involvement of TM6 movement in class B GPCR activation is analogous to the activation mechanism for class A GPCRs. It was first reported that the mutations in the C-terminal portion of the third intracellular loop next to TM6 of β_2AR (32) and α_2AR subtypes (33) cause constitutive activity, leading to an agonist-independent activation of the downstream signaling pathways. Particularly for β_2AR, mutations in the ICL3 loop near TM6 not only caused the receptor to constitutively activate G protein signaling but also promoted the receptor phosphorylation by GPCR kinases and subsequent arrestin recruitment and signaling (32). Both structures of β_2AR complexed with G protein and rhodopsin complexed with arrestin reveal that the outward movement of TM6 is a common feature of an activated GPCR to engage with G protein or arrestin (17, 18). It is likely that the above constitutively active mutations in β_2AR and α_2AR also cause the destabilization of TM6 from the inac-

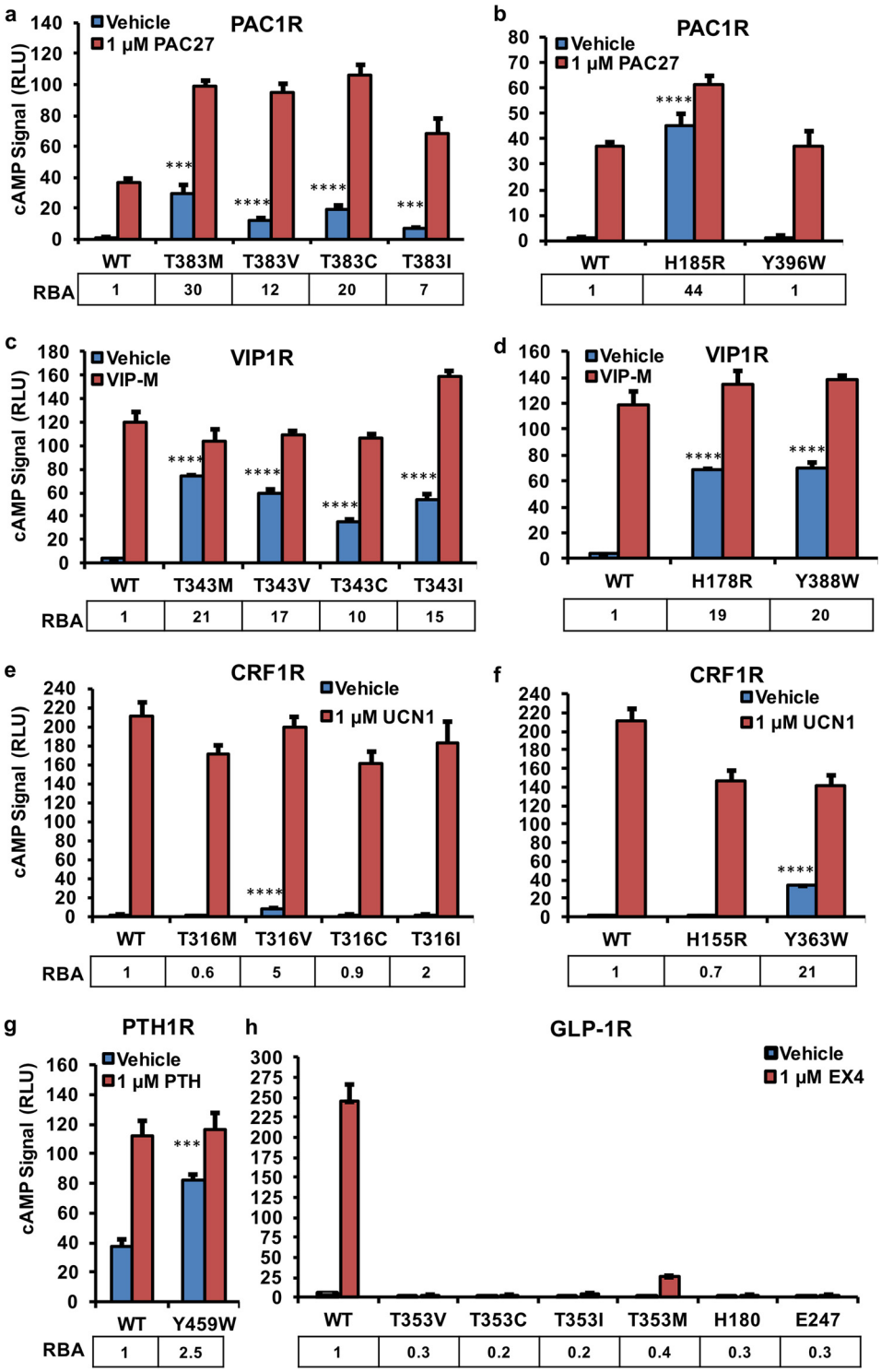

Figure 11. Polar core presents a conserved mechanism for inactivation of class B GPCRs. *a* and *b*, basal and PAC27(1–27)-stimulated cAMP signals produced by full-length PAC1R with amino acid substitutions at positions Thr-383 (*a*) and His-185 and Tyr-396 (*b*). *c* and *d*, basal and membrane-tethered VIP(1–28)-stimulated cAMP signals produced by full-length VIP1R with amino acid substitutions at positions Thr-343 (*c*) and His-178 and Tyr-388 (*d*). *VIP-M*, membrane-tethered VIP(1–28). *e* and *f*, basal and UCN1-stimulated cAMP signal produced by full-length CRF1R with amino acid substitutions at positions Thr-316 (*e*) and His-155 and Tyr-363 (*f*). *g*, basal and parathyroid hormone (*PTH*)-stimulated cAMP signals produced by full-length PTH1R with amino acid substitutions at position Tyr-459. *h*, basal and exendin-4 (*EX4*)-stimulated cAMP signals produced by full-length GLP-1R with amino acid substitutions at position Thr-353, His-180, and Glu-247. Relative basal activity (*RBA*), -fold increase in basal activity of mutated receptors relative to WT receptor. *Error bars* represent S.D. of triplicate determinations. Two-tailed Student's *t* test was used to determine *p* values for data point *versus* the basal activity of the WT receptor: ***, $p \leq 0.001$; ****, $p \leq 0.0001$. *RLU*, relative luciferase unit, which is the ratio of the CRE-luciferase activity to the *Renilla* luciferase activity.

tive conformational state, similar to the mutations in the hydrophobic lock and polar core of class B GPCRs reported here. Based on these data, we thus propose that both class A and class B GPCRs share a common activation mechanism that involves an outward swing of TM6 from the inactive conformational state.

Although both class A and class B GPCRs share a common TM6 activation mechanism, they have distinct interaction networks that keep the receptors in the inactive state. For most class A GPCRs, it is well known that a conserved "ionic lock" formed by a conserved Arg in TM3 and an Asp or Glu in TM6 is the key element that stabilizes the receptor in the inactive state (34, 35). In the case of β_2AR, mutations of these residues increased constitutive activity (35, 36), and biophysical studies have shown that both full and partial agonists can modulate the structure around the ionic lock (37, 38). Thus, the electrostatic interactions between the ionic lock residues play a key role in controlling the movements of TM6 during the activation process. For class B GPCRs, as reported here, the conserved polar core and the GCGR-specific hydrophobic lock keep the receptor in the inactive state. It is reasonable to assume that ligand-induced activation of class B GPCR may also involve rearrangement of the conserved polar core and/or the hydrophobic lock in the case of GCGR.

Even though the polar core is conserved in all members of class B GPCRs, we have noted previously that there is a differential requirement of the receptor ECD for activation of class B GPCRs (16, 24). In the case of GCGR and GLP-1R, the presence of the ECD is required for ligand-mediated activation of the receptor, suggesting an ECD-TMD contact during the receptor activation process. As reported in here, mutations in the GCGR hydrophobic lock and polar core cause constitutive activation regardless of the presence or absence of the ECD, thus suggesting that these mutations can turn the TMD into the active conformation state. In addition, it was reported that the ECD plays a role in repressing the basal activity of GCGR through a putative ECD-TMD interaction (26), and mutations that disrupt this ECD-TMD interaction in GCGR caused a 5-fold higher basal activity (14, 26). However, we failed to reproduce the higher basal activity of the same mutations in our assay system (Fig. 5), and more importantly the mutations in the hydrophobic lock and the polar core of GCGR cause much higher levels of constitutive activities (Figs. 2*a*, 3*a*, 5*a*, 8*a*, and 9), which in some cases exceed activation by a saturated level of ligand, suggesting that these two structural elements play a much more important role in the activation of GCGR.

In summary, we have identified a hydrophobic lock and a polar core next to TM6 as two key structural elements that stabilize the inactive state of GCGR, a prototype member of class B GPCRs. Mutations in either structural element induced constitutive activity of GCGR with the basal level activity of some mutated receptors exceeding the full level of ligand-induced activation of WT receptor. Based on these data, we propose a mechanistic model of GCGR activation in which the TM6 is held in the inactive state by the conserved polar core and the hydrophobic lock, and activation of the receptor must involve an rearrangement of the hydrophobic lock and the polar core. Importantly, mutations in the conserved polar core of PTH1R, PAC1R, VIP1R, and CRF1R also induce constitutive G protein signaling, suggesting that the rearrangement of the polar core could serve as a common mechanism for class B GPCR activation.

Materials and methods

Cloning and mutagenesis

For the cAMP assays, full-length human GCGR (residues 26–443), CRF1R (residues 23–382), PAC1R (residues 21–421), VIP1R (residues 31–457), GLP-1R (residues 24–429), and PTH1R (residues 27–486) were subcloned into pcDNA6 vector. For all receptors, the membrane signal peptide was replaced with an N-terminal human IgG leader sequence (MGWSCIILFLVATATGVHSE) for membrane localization, and a 3×FLAG tag (DYKDDDDKDYKDDDDKDYKDDDDK) was added to their cytoplasmic tails for immunoblotting. The fusion proteins were expressed in AD293 cells. Site-directed mutagenesis experiments were carried out using the QuikChange method (Agilent). Mutations and all plasmid constructs were confirmed by DNA sequencing.

Cell culture

The AD293 or HTL (18, 24) cell lines were routinely grown in Dulbecco's modified Eagle's medium (DMEM) (Invitrogen, Life Technologies) supplemented with 10% (v/v) fetal bovine serum (FBS) (Invitrogen, Life Technologies) in a humidified chamber supplied with 5% CO_2 and 37 °C constant temperature. Cells reaching 80–90% confluence were detached by trypsin and reseeded by 4–6-fold dilution in fresh medium for the assays.

Peptide synthesis

Human GCG(1–29), PAC27(1–27), UCN1(1–40), and exendin-4(1–39) peptides for assays were synthesized and HPLC-purified by Peptide 2. Peptides were dissolved in H_2O (20 mg/ml in stock).

cAMP accumulation assay

AD293 cells were plated at a density of 5×10^4/well in 24-well plates 1 day before transfection. Cells were then transiently transfected using Lipofectamine 2000 reagent (Life Technologies) with 50 ng of cDNA encoding GPCR, 200 ng of CRE-driven fly luciferase reporter and 10 ng of thymidine kinase promoter-driven *Renilla* luciferase, which was used as an internal transfection control at a ratio of 2:1 (Lipofectamine 2000 reagent:DNA). The CRE-luciferase we used here is the pGL4 CRE reporter, originally obtained from Promega as a component of a cAMP assay kit. Detection of cAMP was performed using the Dual-Luciferase reporter assay system from Promega according to the manufacturer's instructions with an EnVision plate reader (PerkinElmer Life Sciences). *Renilla* luciferase was used for normalization. To test the response of the GCGR to exogenous GCG and of VIP1R to exogenous VIP(1–28), we co-expressed 50 ng of membrane-tethered GCG(1–29) plasmid with 50 ng of GCGR and 50 ng of membrane-tethered VIP(1–28) plasmid with 50 ng of VIP1R according to the literature (16, 24). Membrane-tethered GCG(1–29) and VIP(1–28) plasmids refer to the constructs that are the

fusions of glucagon(1–29) and VIP(1–28) to a long flexible linker (a 5×NG linker followed by a MYC tag (EQKLISEEDL), then a 9×NG linker), and the single transmembrane domain of CD8 with sequence ALCWVGIGIGVLAAGVLVVTAIVYVV (25). All experiments were performed in triplicates, each transfected independently.

Cell-based assays for detecting β-arrestin recruitment signaling (Tango assays)

We use HTL cells for the Tango assay. The details of constructs used in this assay are shown below. pcDNA6-based fusion constructs were generated by overlap cloning. From the N to C terminus, the GCGR Tango construct consisted of human IgG leader (MGWSCIILFLVATATGVHSE), GCGR (residues 26–431) in which the flexible C tail is removed, a TEV protease cleavage site, and the transcriptional activator tTA (GPCR-TEV-tTA). The β-arrestin1 Tango construct consisted of preactivated full-length β-arrestin1 with 3A mutation (I386A,V387A,F388A) and fused with TEV protease (β-arrestin1(3A)-TEV protease) at its C terminus. The HTL cells were seeded in 24-well plates (10,000 cells/well). Upon reaching 15–20% confluence, 10 ng of GCGR-TEV-tTA plasmid was co-transfected with 10 ng of β-arrestin1-TEV protease plasmid and 5 ng of phRG-tk *Renilla* luciferase expression vector using X-tremegene (Roche Applied Science) at a ratio of 3:1 (reagent: DNA). Twenty-four hours after transfection, cells were incubated with GCG peptide. For determination of the EC_{50} values of the peptides to the mutated receptors in Tango assays, a series of peptide concentrations ranging from 10 μM to 0.1 pM prepared in DMEM were added to the cells 16 h before collection. Cells were harvested and lysed in Passive Lysis Buffer (Promega). Luciferase assays were performed as stated above.

Surface expression of full-length GCGR

The 293T cells were seeded into a 6-well plate at 6×10^5 cells/well. After overnight culture, the cells were transiently transfected with 4 μg of WT or mutant GCGR DNA using Lipofectamine 2000 transfection reagent. After 24 h, 2×10^5 transfected 293T cells were blocked with PBS containing 5% BSA at room temperature for 15 min and then incubated with 1:100 diluted primary antibody (anti-GCGR, Epitomics, Burlingame, CA) at room temperature for 1 h. The cells were then washed three times with PBS containing 1% BSA followed by a 1-h incubation with anti-rabbit Alexa Fluor 488-conjugated secondary antibody (1:300; Invitrogen) at 4 °C in the dark. After washing, the cells were resuspended in 200 μl of PBS containing 1% BSA for detection in a flow cytometer (Accuri™ C6, BD Biosciences) utilizing laser excitation and emission wavelengths of 488 and 519 nm, respectively. For each measurement, ~20,000 cellular events were collected, and fluorescence intensity of the cell population with positive expression was calculated.

Western blotting for the expression levels of the GCGR with ECD deletion

AD293 cells were split 1 day before transfection at 10^6 cells/well in a 12-well plate. The next day, cells were transfected with 1 μg of GCGR TMD (pcDNA6-GCGR TMD-3×FLAG) using Lipofectamine 2000 (DNA:Lipofectamine 2000 ratio of 1:2). Cells were harvested 24 h later by centrifugation. The supernatant was discarded, and pellets were solubilized in cell lysis reagent (CelLytic M, Sigma) supplemented with 1 mM PMSF and centrifuged at 16,000 × *g* for 10 min. The resulting supernatants mixed with 2× β-mercaptoethanol loading buffer were run on a standard SDS-polyacrylamide gel and transferred to a polyvinylidene fluoride membrane. Membranes were blocked with 5% milk in TBST (20 mM Tris-HCl, pH 8.0, 150 mM NaCl, and 0.05% Tween 20) for 1.5 h and incubated with horseradish peroxidase-conjugated anti-FLAG (Sigma M2) antibody or monoclonal anti-β-actin antibody produced in mouse (clone AC-15, Sigma) followed by anti-mouse HRP for detection. Western blot signal intensities were quantified by integrating the luminosity curve of selected lanes using ImageJ (28). The relative surface expression was calculated using the (target band signal intensities)/(corresponding β-actin signal intensities) relative to WT control.

Statistical analysis

GraphPad Prism software version 5.0 (GraphPad Software Inc., San Diego, CA) was used to fit data to a three-parameter dose-response curve. The statistical significance of all data reported here was determined with Student's *t* test analyses. The column data are presented as means ± S.D., and curve data are presented as mean ± S.E.

Author contributions—Y. Y. and H. E. X. designed the experiments. H. E. X., K. M., and M. W. W. directed the project. Y. Y., Y. H., L. H. Z., D. Y., and X. C. conducted the experiments. Y. Y., P. d. W., Y. J., K. M., and H. E. X. analyzed the results. Y. Y., P. W. d. W., K. M., M. W. W., and H. E. X. wrote the paper with comments from all authors.

References

1. Lagerström, M. C., and Schiöth, H. B. (2008) Structural diversity of G protein-coupled receptors and significance for drug discovery. *Nat. Rev. Drug Discov.* **7,** 339–357
2. Hancock, A. S., Du, A., Liu, J., Miller, M., and May, C. L. (2010) Glucagon deficiency reduces hepatic glucose production and improves glucose tolerance in adult mice. *Mol. Endocrinol.* **24,** 1605–1614
3. Kumar, S., Pioszak, A., Zhang, C., Swaminathan, K., and Xu, H. E. (2011) Crystal structure of the PAC1R extracellular domain unifies a consensus fold for hormone recognition by class B G-protein coupled receptors. *PLoS One* **6,** e19682
4. Hoare, S. R. (2005) Mechanisms of peptide and nonpeptide ligand binding to Class B G-protein-coupled receptors. *Drug Discov. Today* **10,** 417–427
5. Parthier, C., Reedtz-Runge, S., Rudolph, R., and Stubbs, M. T. (2009) Passing the baton in class B GPCRs: peptide hormone activation via helix induction? *Trends Biochem. Sci.* **34,** 303–310
6. Grace, C. R., Perrin, M. H., DiGruccio, M. R., Miller, C. L., Rivier, J. E., Vale, W. W., and Riek, R. (2004) NMR structure and peptide hormone binding site of the first extracellular domain of a type B1 G protein-coupled receptor. *Proc. Natl. Acad. Sci. U.S.A.* **101,** 12836–12841
7. Wittelsberger, A., Corich, M., Thomas, B. E., Lee, B.-K., Barazza, A., Czodrowski, P., Mierke, D. F., Chorev, M., and Rosenblatt, M. (2006) The mid-region of parathyroid hormone (1–34) serves as a functional docking domain in receptor activation. *Biochemistry* **45,** 2027–2034
8. Hennen, S., Kodra, J. T., Soroka, V., Krogh, B. O., Wu, X., Kaastrup, P., Ørskov, C., Rønn, S. G., Schluckebier, G., Barbateskovic, S., Gandhi, P. S., and Reedtz-Runge, S. (2016) Structural insight into antibody-mediated antagonism of the glucagon-like peptide-1 receptor. *Sci. Rep.* **6,** 26236

9. Pal, K., Melcher, K., and Xu, H. E. (2012) Structure and mechanism for recognition of peptide hormones by class B G-protein-coupled receptors. *Acta Pharmacol. Sin.* **33,** 300–311
10. Pioszak, A. A., Parker, N. R., Suino-Powell, K., and Xu, H. E. (2008) Molecular recognition of corticotropin-releasing factor by its G-protein-coupled receptor CRFR1. *J. Biol. Chem.* **283,** 32900–32912
11. Siu, F. Y., and Stevens, R. C. (2010) RAMP-ing up class-B GPCR ECD structural coverage. *Structure* **18,** 1067–1068
12. Jazayeri, A., Doré, A. S., Lamb, D., Krishnamurthy, H., Southall, S. M., Baig, A. H., Bortolato, A., Koglin, M., Robertson, N. J., Errey, J. C., Andrews, S. P., Teobald, I., Brown, A. J., Cooke, R. M., Weir, M., *et al.* (2016) Extra-helical binding site of a glucagon receptor antagonist. *Nature* **533,** 274–277
13. Siu, F. Y., He, M., de Graaf, C., Han, G. W., Yang, D., Zhang, Z., Zhou, C., Xu, Q., Wacker, D., Joseph, J. S., Liu, W., Lau, J., Cherezov, V., Katritch, V., Wang, M.-W., and Stevens, R. C. (2013) Structure of the human glucagon class B G-protein-coupled receptor. *Nature* **499,** 444–449
14. Yang, L., Yang, D., de Graaf, C., Moeller, A., West, G. M., Dharmarajan, V., Wang, C., Siu, F. Y., Song, G., Reedtz-Runge, S., Pascal, B. D., Wu, B., Potter, C. S., Zhou, H., Griffin, P. R., *et al.* (2015) Conformational states of the full-length glucagon receptor. *Nat. Commun.* **6,** 7859
15. Koth, C. M., Murray, J. M., Mukund, S., Madjidi, A., Minn, A., Clarke, H. J., Wong, T., Chiang, V., Luis, E., Estevez, A., Rondon, J., Zhang, Y., Hötzel, I., and Allan, B. B. (2012) Molecular basis for negative regulation of the glucagon receptor. *Proc. Natl. Acad. Sci. U.S.A.* **109,** 14393–14398
16. Zhao, L.-H., Yin, Y., Yang, D., Liu, B., Hou, L., Wang, X., Pal, K., Jiang, Y., Feng, Y., Cai, X., Dai, A., Liu, M., Wang, M., Melcher, K., and Xu, H. E. (2016) Differential requirement of the extracellular domain in activation of class B G protein-coupled receptors. *J. Biol. Chem.* **291,** 15119–15130
17. Rasmussen, S. G., DeVree, B. T., Zou, Y., Kruse, A. C., Chung, K. Y., Kobilka, T. S., Thian, F. S., Chae, P. S., Pardon, E., Calinski, D., Mathiesen, J. M., Shah, S. T., Lyons, J. A., Caffrey, M., Gellman, S. H., *et al.* (2011) Crystal structure of the β2 adrenergic receptor-Gs protein complex. *Nature* **477,** 549–555
18. Kang, Y., Zhou, X. E., Gao, X., He, Y., Liu, W., Ishchenko, A., Barty, A., White, T. A., Yefanov, O., Han, G. W., Xu, Q., de Waal, P. W., Ke, J., Tan, M. H., Zhang, C., *et al.* (2015) Crystal structure of rhodopsin bound to arrestin by femtosecond X-ray laser. *Nature.* **523,** 561–567
19. Ward, S. D., Hamdan, F. F., Bloodworth, L. M., and Wess, J. (2002) Conformational changes that occur during M_3 muscarinic acetylcholine receptor activation probed by the use of an *in situ* disulfide cross-linking strategy. *J. Biol. Chem.* **277,** 2247–2257
20. Ward, S. D., Hamdan, F. F., Bloodworth, L. M., Siddiqui, N. A., Li, J. H., and Wess, J. (2006) Use of an *in situ* disulfide cross-linking strategy to study the dynamic properties of the cytoplasmic end of transmembrane domain VI of the M_3 muscarinic acetylcholine receptor. *Biochemistry* **45,** 676–685
21. Han, S.-J., Hamdan, F. F., Kim, S.-K., Jacobson, K. A., Bloodworth, L. M., Li, B., and Wess, J. (2005) Identification of an agonist-induced conformational change occurring adjacent to the ligand-binding pocket of the M_3 muscarinic acetylcholine receptor. *J. Biol. Chem.* **280,** 34849–34858
22. Kobilka, B. K. (2007) G protein coupled receptor structure and activation. *Biochim. Biophys. Acta* **1768,** 794–807
23. Nolte, W. M., Fortin, J.-P., Stevens, B. D., Aspnes, G. E., Griffith, D. A., Hoth, L. R., Ruggeri, R. B., Mathiowetz, A. M., Limberakis, C., Hepworth, D., and Carpino, P. A. (2014) A potentiator of orthosteric ligand activity at GLP-1R acts via covalent modification. *Nat. Chem. Biol.* **10,** 629–631
24. Yin, Y., Zhou, X. E., Hou, L., Zhao, L.-H., Liu, B., Wang, G., Jiang, Y., Melcher, K., and Xu, H. E. (2016) An intrinsic agonist mechanism for activation of glucagon-like peptide-1 receptor by its extracellular domain. *Cell Discov.* **2,** 16042
25. Fortin, J.-P., Zhu, Y., Choi, C., Beinborn, M., Nitabach, M. N., and Kopin, A. S. (2009) Membrane-tethered ligands are effective probes for exploring class B1 G protein-coupled receptor function. *Proc. Natl. Acad. Sci. U.S.A.* **106,** 8049–8054
26. Mukund, S., Shang, Y., Clarke, H. J., Madjidi, A., Corn, J. E., Kates, L., Kolumam, G., Chiang, V., Luis, E., Murray, J., Zhang, Y., Hötzel, I., Koth, C. M., and Allan, B. B. (2013) Inhibitory mechanism of an allosteric antibody targeting the glucagon receptor. *J. Biol. Chem.* **288,** 36168–36178
27. Pabreja, K., Mohd, M. A., Koole, C., Wootten, D., and Furness, S. G. (2014) Molecular mechanisms underlying physiological and receptor pleiotropic effects mediated by GLP-1R activation. *Br. J. Pharmacol.* **171,** 1114–1128
28. Schneider, C. A., Rasband, W. S., and Eliceiri, K. W. (2012) NIH Image to ImageJ: 25 years of image analysis. *Nat. Methods.* **9,** 671–675
29. Nampoothiri, S., Fernández-Rebollo, E., Yesodharan, D., Gardella, T. J., Rush, E. T., Langman, C. B., and Jüppner, H. (2016) Jansen metaphyseal chondrodysplasia due to heterozygous H223R-PTH1R mutations with or without overt hypercalcemia. *J. Clin. Endocrinol. Metab.* **101,** 4283–4289
30. Schipani, E., Jensen, G. S., Pincus, J., Nissenson, R. A., Gardella, T. J., and Jüppner, H. (1997) Constitutive activation of the cyclic adenosine 3′,5′-monophosphate signaling pathway by parathyroid hormone (PTH)/PTH-related peptide receptors mutated at the two loci for Jansen's metaphyseal chondrodysplasia. *Mol. Endocrinol.* **11,** 851–858
31. Hjorth, S. A., Orskov, C., and Schwartz, T. W. (1998) Constitutive activity of glucagon receptor mutants. *Mol. Endocrinol.* **12,** 78–86
32. Pei, G., Samama, P., Lohse, M., Wang, M., Codina, J., and Lefkowitz, R. J. (1994) A constitutively active mutant β2-adrenergic receptor is constitutively desensitized and phosphorylated. *Proc. Natl. Acad. Sci. U.S.A.* **91,** 2699–2702
33. Ren, Q., Kurose, H., Lefkowitz, R. J., and Cotecchia, S. (1993) Constitutively active mutants of the α_2-adrenergic receptor. *J. Biol. Chem.* **268,** 16483–16487
34. Vogel, R., Mahalingam, M., Lüdeke, S., Huber, T., Siebert, F., and Sakmar, T. P. (2008) Functional role of the "ionic lock"—an interhelical hydrogen-bond network in family A heptahelical receptors. *J. Mol. Biol.* **380,** 648–655
35. Ballesteros, J. A., Jensen, A. D., Liapakis, G., Rasmussen, S. G., Shi, L., Gether, U., and Javitch, J. A. (2001) Activation of the β_2-adrenergic receptor involves disruption of an ionic lock between the cytoplasmic ends of transmembrane segments 3 and 6. *J. Biol. Chem.* **276,** 29171–29177
36. Rasmussen, S. G., Jensen, A. D., Liapakis, G., Ghanouni, P., Javitch, J. A., and Gether, U. (1999) Mutation of a highly conserved aspartic acid in the β2 adrenergic receptor: constitutive activation, structural instability, and conformational rearrangement of transmembrane segment 6. *Mol. Pharmacol.* **56,** 175–184
37. Yao, X., Parnot, C., Deupi, X., Ratnala, V. R., Swaminath, G., Farrens, D., and Kobilka, B. (2006) Coupling ligand structure to specific conformational switches in the β2-adrenoceptor. *Nat. Chem. Biol.* **2,** 417–422
38. Mason, J. S., Bortolato, A., Congreve, M., and Marshall, F. H. (2012) New insights from structural biology into the druggability of G protein-coupled receptors. *Trends Pharmacol. Sci.* **33,** 249–260